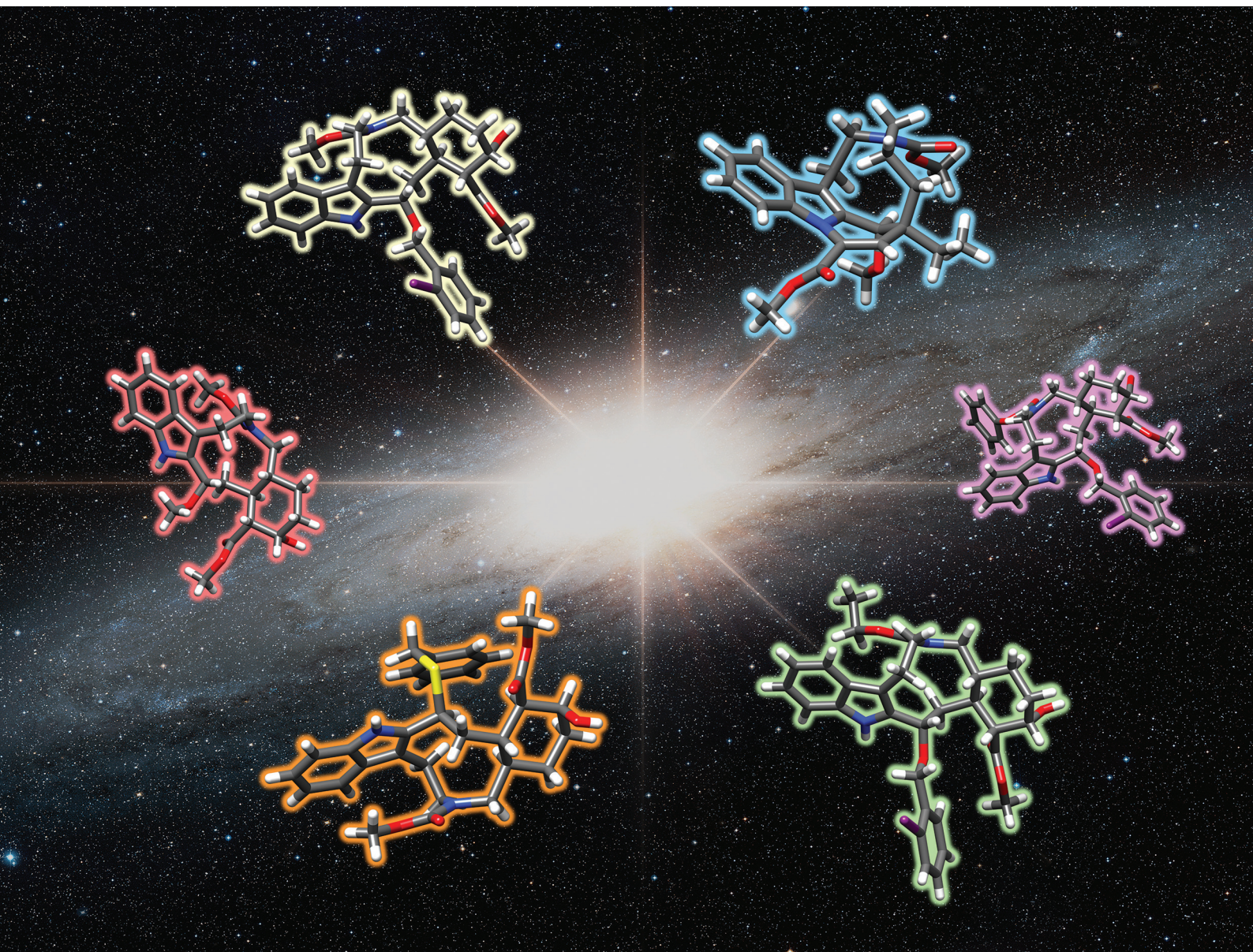


Organic & Biomolecular Chemistry

Volume 22
Number 42
14 November 2024
Pages 8357-8518

rsc.li/obc



ISSN 1477-0520

PAPER

Robert W. Huigens III *et al.*
Chloroformate-mediated ring cleavage of indole alkaloids
leads to re-engineered antiplasmodial agents

Cite this: *Org. Biomol. Chem.*, 2024, **22**, 8423

Chloroformate-mediated ring cleavage of indole alkaloids leads to re-engineered antiplasmodial agents†

Daniel C. Schultz,^{‡a} Alejandra Chávez-Riveros,^{‡a} Michael G. Goertzen, II,^a Beau R. Brummel,^a Raphaella A. Paes,^b Natalia M. Santos,^b Srinivasarao Tenneti,^a Khalil A. Abboud,^c James R. Rocca,^{a,d} Gustavo Seabra,^a Chenglong Li,^a Debopam Chakrabarti^b and Robert W. Huigens III^{*,a}

Natural product ring distortion strategies have enabled rapid access to unique libraries of stereochemically complex compounds to explore new chemical space and increase our understanding of biological processes related to human disease. Herein is described the development of a ring-cleavage strategy using the indole alkaloids yohimbine, apovincamine, vinburnine, and reserpine that were reacted with a diversity of chloroformates paired with various alcohol/thiol nucleophiles to enable the rapid synthesis of 47 novel small molecules. Ring cleavage reactions of yohimbine and reserpine produced two diastereomeric products in moderate to excellent yields, whereas apovincamine and vinburnine produced a single diastereomeric product in significantly lower yields. Free energy calculations indicated that diastereoselectivity regarding select ring cleavage reactions from yohimbine and apovincamine is dictated by the geometry and three-dimensional structure of reactive cationic intermediates. These compounds were screened for antiplasmodial activity due to the need for novel antimalarial agents. Reserpine derivative **41** was found to exhibit interesting antiplasmodial activities against *Plasmodium falciparum* parasites (EC₅₀ = 0.50 μM against Dd2 cultures), while its diastereomer **40** was found to be three-fold less active (EC₅₀ = 1.78 μM). Overall, these studies demonstrate that the ring distortion of available indole alkaloids can lead to unique compound collections with re-engineered biological activities for exploring and potentially treating human disease.

Received 22nd May 2024,
Accepted 26th June 2024

DOI: 10.1039/d4ob00853g

rsc.li/obc

Introduction

Complexity-to-Diversity (CtD) strategies to explore chemical space have gained traction as a means to generate novel, structurally diverse, and stereochemically complex compound libraries from select natural products.^{1–16} The CtD strategy relies on chemoselective “ring distortion” reactions to rapidly alter the molecular skeleton of various natural products

bearing fused ring systems to access diverse compounds of high stereochemical complexity. The CtD synthesis approach has been successfully applied to multiple natural products to date, including: adrenosterone,¹ gibberellic acid,¹ quinine,¹ pleuromutilin,^{2,15} abietic acid,⁹ sinomenine,¹⁰ yohimbine,^{3,6,7,11} lycorine,¹² vincamine,^{4,8,16} and other steroids.^{13,14} The overarching goal of CtD (or “ring distortion”) is to access diverse molecular scaffolds to discover compounds with re-engineered biological activities in critical disease areas. CtD offers an orthogonal discovery approach to diversity-oriented synthesis (DOS; simple materials utilized in complexity-generating reactions)^{17–24} and biology-oriented synthesis (BIOS; generation of natural product-like molecules based on cheminformatic analysis of natural products and conserved proteins).^{25–32} Noteworthy examples of the CtD platform delivering re-engineered small molecules include the discovery of vincamine-derived **V2a**, which demonstrates antagonistic activity against hypocretin receptor 2 and inhibits morphine-seeking behaviors in mouse models,¹⁶ and the identification of pleuromutilin-derived ferroptocid, a thioredoxin inhibitor

^aDepartment of Medicinal Chemistry, Center for Natural Product Drug Discovery & Development (CNPd3), College of Pharmacy, University of Florida, Gainesville, Florida 32610, USA. E-mail: rhuigens@cop.ufl.edu

^bDivision of Molecular Microbiology, Burnett School of Biomedical Sciences, University of Central Florida, Orlando, Florida 32826, USA

^cDepartment of Chemistry, University of Florida, Gainesville, Florida 32610, USA

^dMcKnight Brain Institute, J H Miller Health Center, University of Florida, Gainesville, Florida 32610, USA

† Electronic supplementary information (ESI) available. CCDC 2337941 2338890 2338892 2338891 2338909 2338889. For ESI and crystallographic data in CIF or other electronic format see DOI: <https://doi.org/10.1039/d4ob00853g>

‡ These authors contributed equally to this work.

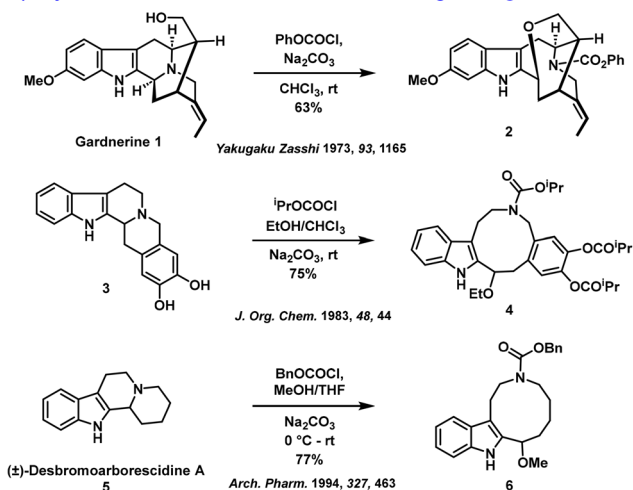
that positively modulates the immune system in a murine model of breast cancer.¹⁵

Chloroformate-mediated ring cleavage of gardnerine **1** and derivatives was reported by Sakai and colleagues in 1973 (Fig. 1A).³³ In this reaction type, a polycyclic tryptoline system containing a tertiary amine is reacted with a chloroformate electrophile in the presence of an alcohol nucleophile, leading to an indole-promoted ring cleavage and the incorporation of carbamate and ether moieties. This methodology has been applied to a few indole alkaloids and related scaffolds, with notable examples in Fig. 1A (*e.g.*, (\pm)-desbromoarborescidine **5**).^{34–36} The versatility of this reaction to diversity at two positions of the tryptoline framework while performing a regioselective ring cleavage proved an attractive strategy to expand our ring distortion platform using multiple indole alkaloids. Additionally, our previous ring distortion efforts with yohimbine and vincamine involving alternative ring cleavage methods resulted in the discovery of Nrf2-Antioxidant Response Element (ARE) inhibitor

Y6q and antiplasmodial agent **V3b** (Fig. 1B, structures **8** & **10**);^{4,11} therefore, we hypothesized that reacting chloroformates and alcohols/thiols with indole alkaloids would yield interesting ring-cleaved compounds with re-engineered biological activities.

During the course of these studies, multiple indole alkaloids were subjected to chloroformate-mediated indole-promoted ring cleavage reactions to access 47 new analogues. Nearly all ring-cleaved analogues synthesized proved to be challenging to characterize by standard NMR conditions due to the resulting medium-sized ring bearing a carbamate functional group. This robust methodology resulted in new stereochemically complex indole-containing small molecules bearing diversity elements in two positions (new carbamate and ether/thioether). Ring cleavage reactions from yohimbine and reserpine produced a mixture of diastereomeric products, while reactions from apovincamine/vinburnine produced a single diastereomeric product. Free energy calculations were used to study the energetics of this transformation from yohimbine and apovincamine. Finally, this new collection of compounds was screened against the malarial parasite *Plasmodium falciparum* to discover new antiplasmodial agents with re-engineered activities from reserpine.

A) Key Indole-Promoted Chloroformate-Mediated Ring Cleavage Reactions



B) Re-Engineering Indole Alkaloid Activity Through Ring Cleavage

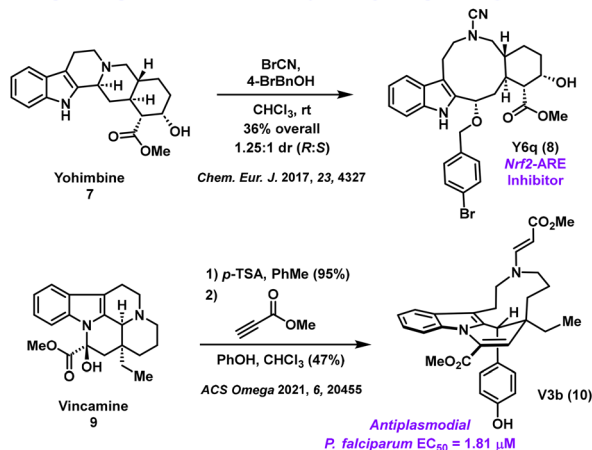


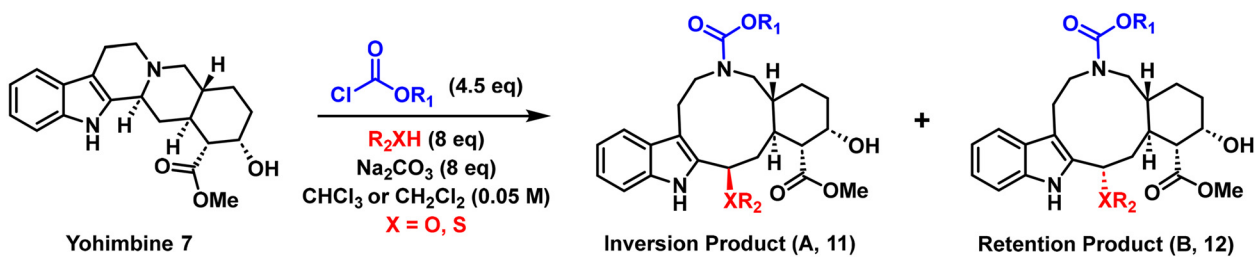
Fig. 1 Reported examples of indole-promoted ring cleavage reactions. (A) Select literature precedents for indole-promoted ring cleavage using chloroformates and alcohols. (B) Re-engineered indole alkaloid derivatives accessed through ring cleavage methods.

Results and discussion

Indole-promoted ring cleavage of yohimbine with diverse chloroformates and alcohols/thiols

Our initial experiments subjected yohimbine **7** (free base) to phenyl chloroformate and methanol in chloroform at 60 °C for three hours to afford a mixture of products at a 1.2 : 1 diastereomeric ratio (dr) in 96% combined yield (Fig. 2A, entry 1; general diastereomeric products are referred to the “inversion product” **11** and “retention product” **12**). Encouraged by the excellent yield and separability of the target diastereomers using column chromatography, the scope of this reaction was explored with yohimbine **7** to assess six chloroformate electrophiles and six alcohol or thiol nucleophiles (Fig. 2A & ESI Table 2† for additional experimental details). Collectively, these efforts afforded fourteen diastereomeric product pairs ranging from 33–96% combined yields with diastereomeric ratios of 1 : 1 to 1 : 3 (inversion product **11** to retention product **12**). To probe reaction performance, ring cleavage reactions of **7** were typically carried out at (1) room temperature, (2) 60 °C in an oil bath, or (3) 60 °C in a microwave reactor. Reactions performed on yohimbine **7** at room temperature generally required more time to complete compared to reactions heated in an oil bath; however, microwave heated reactions were completed in 15 minutes. Interestingly, reactions demonstrating some diastereoselectivity had the retention product **12** as the major product in nearly all cases. In general, bulkier nucleophiles tended to produce lower overall yields of the desired products upon reaction with yohimbine and chloroformates (*e.g.*, Fig. 2A, entry 4, *tert*-butanol produced 33% combined yield of diastereomeric products); however, higher diastereoselectivities were observed.

A) Chloroformate-Mediated Ring Cleavage of Yohimbine



28 Total Compounds Synthesized

Conditions	E^{\oplus}	Nuc:	Time	Percent Yield (Isolated Yield A / B)
1) $CHCl_3$, 60 °C, oil bath	$ClCO_2Ph$	MeOH	3 h	96% combined yield (53% A / 43% B)
2) $CHCl_3$, 60 °C, microwave	$ClCO_2Ph$	2-I-BnOH	15 min	75% combined yield (21% A / 54% B)
3) $CHCl_3$, room temp.	$ClCO_2Ph$	BnSH	9 h	67% combined yield (32% A / 35% B)
4) $CHCl_3$, 60 °C, oil bath	$ClCO_2Ph$	^t BuOH	3 h	33% combined yield (13% A / 20% B)
5) CH_2Cl_2 , room temp.	$ClCO_2Ph$	2-Butyn-1-ol	3 h	89% combined yield (27% A / 62% B)
6) $CHCl_3$, 60 °C, oil bath	$ClCO_2Me$	MeOH	1 h	90% combined yield (39% A / 51% B)
7) $CHCl_3$, room temp.	$ClCO_2Me$	EtSH	18 h	44% combined yield (11% A / 33% B)
8) $CHCl_3$, 60 °C, oil bath	$ClCO_2Me$	2-I-BnOH	20 h	45% combined yield (17% A / 28% B)
9) $CHCl_3$, 60 °C, oil bath	$ClCO_2Me$	BnSH	3 h	50% combined yield (23% A / 27% B)
10) $CHCl_3$, 60 °C, oil bath	$ClCO_2Et$	MeOH	3 h	81% combined yield (41% A / 40% B)
11) $CHCl_3$, 60 °C, microwave	$ClCO_2Et$	2-I-BnOH	15 min	49% combined yield (18% A / 31% B)
12) $CHCl_3$, 60 °C, oil bath	$ClCO_2CH_2CCl_3$	MeOH	3 h	87% combined yield (38% A / 49% B)
13) $CHCl_3$, room temp.	$ClCO_2CH_2CH=CH_2$	MeOH	4 h	60% combined yield (29% A / 31% B)
14) $CHCl_3$, room temp.	$ClCO_2CH_2C\equiv CH$	MeOH	5 h	52% combined yield (18% A / 34% B)

B) Key NOEs for Stereochemical Assignment at C3 of Yohimbine Products

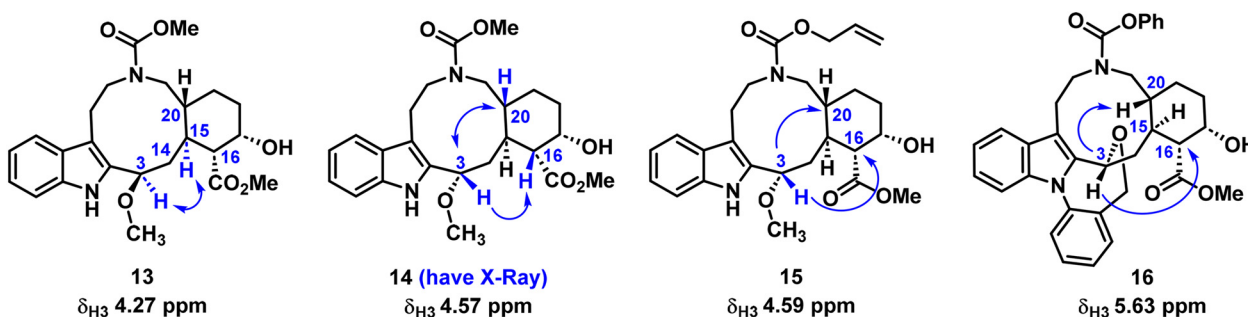


Fig. 2 (A) Indole-promoted ring cleavage of yohimbine yields diastereomeric products 11 and 12. (B) NOEs utilized to determine the stereochemistry of ring-cleavage products from yohimbine.

We found the ring cleavage of yohimbine **7** to be a remarkable transformation as the chloroformate and alcohol/thiol in the reaction could react together without yohimbine's involvement to produce undesired materials. These reactions proved incredibly chemoselective as the tertiary amine of yohimbine **7** first reacts with the electrophilic chloroformate to generate an activated *N*-acyl ammonium intermediate that then undergoes an indole-promoted ring cleavage to form a resonance-stabilized carbocation, which is reacted with the alcohol/thiol nucleophile in the final step to produce the diastereomeric products **11** and **12**. Exploration of this reaction-type was further probed to assess the tolerance of this ring cleavage transformation in the presence of alternative electrophiles, nucleophiles, and solvents. We found the electrophilic character of chloroformates to be requisite for reaction progression, as our attempts involving sulfonyl chlorides and acyl chlorides did not proceed. Similarly, reactions employing non-alcohol or thiol nucleophiles, such as benzoic acid, trimethylsilyl azide, and tosyl amide, were met with failure. Additionally, similar ring cleavage reactions using solely chloroformates (*i.e.*, the displaced chloride serving as the nucleophile) have been reported with other indole-containing compounds bearing a tryptoline motif,³⁷ however, attempts to perform this reaction with yohimbine **7** in the absence of an alcohol/thiol nucleophile proved unsuccessful. Solvent selection was also found to be critical for the desired indole-promoted ring cleavage transformation to occur, as no reaction with yohimbine was observed in tetrahydrofuran, toluene, or acetone. Chloroform and dichloromethane were the sole tested solvents that led to the successful ring cleavage of yohimbine **7** (see Fig. 2A).

The absolute stereochemical assignment of the diastereomeric products from yohimbine **7** proved to be non-trivial due to the nature of the medium-sized ring bearing a carbamate. The diastereomeric pairs from yohimbine **7** were characterized using NMR and X-ray analysis to support and confirm chemical shift trends observed among this series (see Fig. 2B for select cases; the "inversion product" had the chemical shift of H3 upfield relative to the H3 proton signal in the "retention product" based on ¹H NMR studies conducted in C₂D₂Cl₄; the only exception being diastereomers **23** and **24**, which were the only products where NMRs were taken in DMSO-*d*₆; see Fig. 3, and ESI Table 1†). These observations aligned with previous work by our lab^{4,11} and others^{38–40} requiring variable temperature NMR to characterize medium-size ring compounds. High temperature NMR experiments were required to produce well-resolved signals (peaks) as we believe the ring-cleaved products from yohimbine exist as a mixture of slowly interconverting conformers and/or mixtures of rotamers at the carbamate moiety at room temperature which produce distinct but often broad or nonexistent signals in NMR spectra (see ESI Fig. 3†). After performing NMR experiments at 100 °C in C₂D₂Cl₄, however, interconversion between conformers/rotamers occurred at an adequate rate such that previously distinct peaks coalesced, and broad, weak peaks became sharper, allowing for definitive structural elucidation (see ESI†). While this trend was generally met with success across the diastereo-

meric products synthesized from yohimbine, there were select instances where peaks remained broad or unobservable.

Prior to the acquisition of high-quality crystals for X-ray diffraction to unambiguously assign stereochemistry at the C3 position of yohimbine-derived ring cleavage products (*i.e.*, analogues of general structure **11** and **12**), stereochemical assignments were made using selective one-dimensional nuclear Overhauser effect spectroscopy (NOESY; Fig. 2B & ESI†). Upon irradiation of the H3 of inversion product **13**, a through-space NOE was observed by the C15 methine (Fig. 2B & 3). In addition, a NOESY correlation is also observed in the reverse direction regarding **13**, following irradiation of H15 (which NOEs to H3), confirming that H3 of **13** is on the same face of the newly formed medium sized ring as H15. Conversely, upon irradiation of the H3 methine of **14**, an NOE was observed with H20 and H16, which are *anti* to H15, indicating the stereochemistry correlates to the retention product (Fig. 2B). The absolute stereochemistry of **14** was further validated by X-ray analysis (Fig. 3), which aligned with our NOE findings. Similar NOE profiles were observed for products **15** and **16** (Fig. 2B).

Using the chloroformate and alcohol/thiol ring cleavage reaction, we were able to collectively synthesize 28 new compounds (14 diastereomeric pairs) from yohimbine **7**. From this focused series of diastereomeric product pairs, an observable trend in chemical shifts at H3 was clear between the inversion **11** and retention **12** products, allowing us to assign stereochemistry for all synthetic analogues. As demonstrated in Fig. 3, the δ_{H3} for the inversion products were typically observed to be 0.3–0.5 ppm upfield (*e.g.*, **13**, **17**, **19**, **21**) when compared to the corresponding retention product diastereomers (*e.g.*, **14**, **18**, **20**, **22**). We observed a similar trend in previous studies with the cyanogen bromide-mediated ring cleavage of yohimbine¹¹ (ESI Table 1†). The lone exception we observed during this study can be seen in the chemical shifts of thioether diastereomers **23** and **24** (Fig. 3; we obtained an X-ray of **24**); however, we attribute this result from being the only diastereomeric pair that used DMSO-*d*₆ in NMR experiments. Interestingly, five retention products synthesized from yohimbine readily produced high-quality single crystals suitable for X-ray diffraction studies whereas we were unable to produce any crystals of inversion products for X-ray analysis despite multiple attempts.

The chloroformate-mediated ring cleavage of yohimbine not only enabled rapid access to a focused series of analogues, but also allowed for further synthetic transformations to expand the diversity of compounds accessed through this method (see ESI Fig. 5†). Select yohimbine ring-cleaved compounds were subjected to the removal of carbamate functional groups to yield the corresponding secondary amine that could be acylated. In addition, the indole nitrogen and secondary alcohol of a select yohimbine analogue were methylated using Williamson ether synthesis conditions while another analogue was subjected to an intramolecular copper-catalyzed C–N coupling between the indole nitrogen and aryl iodide installed in the ring cleavage reaction to access ring fusion compound **16**. Overall, the chloroformate-mediated ring cleavage of yohim-

X-Rays of Yohimbine Products Support NMR Trends for Stereochemical Assignment

Inversion Product (A)

Retention Product (B) with X-Ray

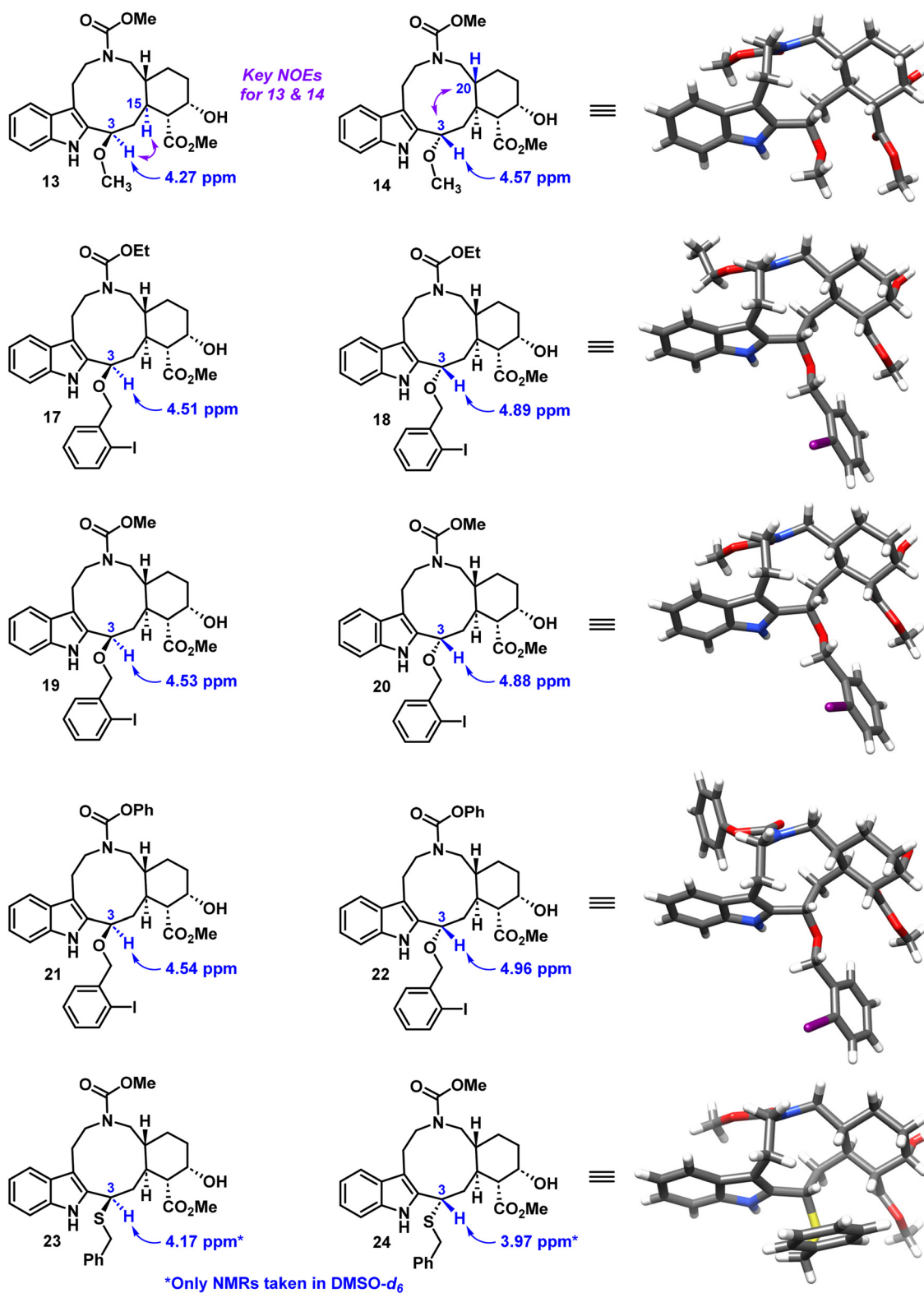


Fig. 3 X-Rays of "retention products" synthesized from yohimbine aided in the stereochemical assignment of diastereomeric pairs generated during these studies.

bine proved to be a robust transformation leading to the synthesis of 33 new derivatives (see ESI Fig. 1†).

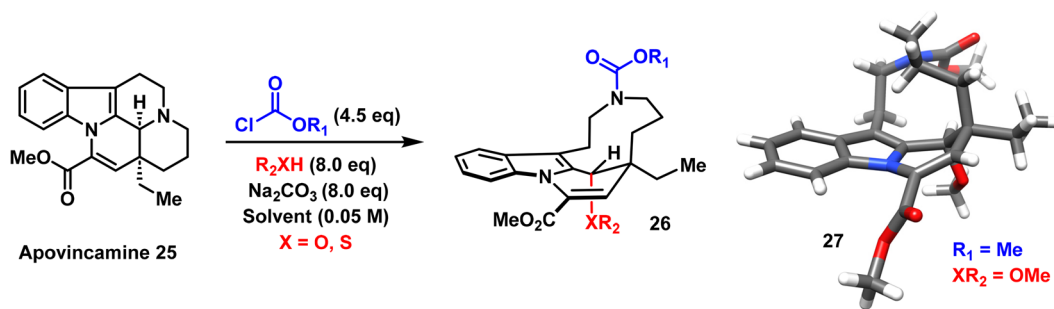
Indole-promoted ring cleavage of apovincamine and vinburnine

In parallel studies, we performed chloroformate-mediated ring cleavage reactions on vincamine-derived compounds apovincamine 25 and vinburnine 28 (Fig. 4). Vincamine can be purchased on decagram scale and readily converted to apovincamine and vinburnine,^{4,16} which was critical for these efforts as the ring cleavage reactions on 25 and 28 were significantly lower yielding (*i.e.*, 4–67% yield) when compared to our yohimbine studies. We believe the additional ring fused onto the indole heterocycle of these vincamine-derived substrates negatively impacted the efficiency of this ring cleavage transform-

ation. Despite these challenges, we were able to synthesize 12 new ring-cleaved analogues from 25 and 28 using a diversity of chloroformates with alcohols/thiols.

Ring cleavage reactions with apovincamine 25 required harsh conditions (*e.g.*, 100 °C *via* microwave irradiation for one hour, or in a sealed tube for days) and typically gave poor yields with significant amounts of starting material following the end of the reaction (with up to 76% starting material recovered following reaction; see ESI Table 3†). For these reactions, dichloromethane was found to be superior to chloroform as a reaction solvent. Despite low yields, all ring cleavage reactions with 25 and 28 produced a single diastereomeric product which we characterize as the inversion product based on the X-ray of derivative 27 (Fig. 4). Based on the molecular architecture of the resonance-stabilized

Chloroformate Ring Cleavage of Apovincamine and Vinburnine



Conditions	E ⁺	Nuc:	Time	Percent Yield
1) CH ₂ Cl ₂ , 100 °C, microwave	ClCO ₂ Me	MeOH	1 h	35% yield
2) CH ₂ Cl ₂ , 100 °C, sealed tube	ClCO ₂ Et	MeOH	68 h	67% yield
3) CHCl ₃ , 100 °C, microwave	ClCO ₂ Ph	MeOH	1 h	6% yield
4) CHCl ₃ , 100 °C, microwave	ClCO ₂ CH ₂ CCl ₃	MeOH	1 h	21% yield
5) CHCl ₃ , 100 °C, microwave	ClCO ₂ CH ₂ CH=CH ₂	MeOH	1 h	10% yield
6) CHCl ₃ , 100 °C, microwave	ClCO ₂ Me	EtOH	1 h	30% yield
7) CHCl ₃ , 100 °C, microwave	ClCO ₂ Me	Propargyl alcohol	1 h	16% yield
8) CH ₂ Cl ₂ , 100 °C, microwave	ClCO ₂ Me	2-Butyn-1-ol	1 h	17% yield
9) CH ₂ Cl ₂ , 100 °C, microwave	ClCO ₂ Me	Allyl alcohol	1 h	51% yield
10) CH ₂ Cl ₂ , 100 °C, microwave	ClCO ₂ Me	BnOH	1 h	24% yield
11) CH ₂ Cl ₂ , 100 °C, microwave	ClCO ₂ Me	EtSH	1 h	25% yield

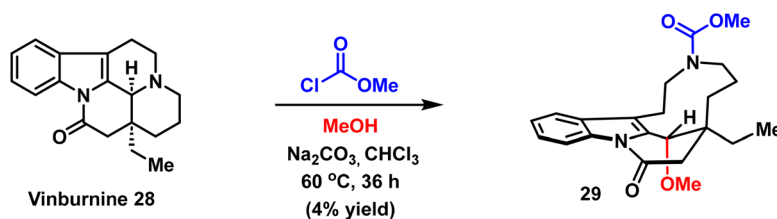


Fig. 4 Chloroformate-mediated ring cleavage of apovincamine 25 and vinburnine 28 with various alcohol and thiol nucleophiles to give single diastereomer products (*e.g.*, 27 which has X-ray included).

intermediate that forms directly after C–N bond cleavage, subsequent nucleophilic attack from the alcohol/thiol nucleophile would be expected on the opposite face of the new carbamate to yield the desired product as a single diastereomer (computational studies support this notion and are detailed in a later section). The close proximity of the newly formed carbamate to the highly electrophilic carbon center generated during the course of the reaction also explains why significant amounts of starting materials are present at the end of the reaction as we believe the indole-stabilized intermediate can readily convert back to starting material. In addition, vinburnine **28** was found to be a very poor substrate for chloroformate-mediated ring-cleavage reactions. This finding was not overly surprising as vinburnine's indole nitrogen is part of an amide functionality; therefore, the indole system of **28** is more electron deficient and not primed to facilitate chemistry that relies on the formation of an indole-stabilized carbocation. Despite several failed reactions with vinburnine **28**, we were able to use methyl chloroformate in combination with methanol to obtain the desired ring-cleaved product **29** in 4% yield (TLC analysis showed very little vinburnine **28** reacting despite elevated temperatures in an oil bath for 36 hours; Fig. 4).

Computational analysis of yohimbine and apovincamine ring cleavage reactions

Density functional theory calculations were pursued through Gaussian^{41,42} (Functional: M06-2X;⁴³ Basis sets: 6-311G++(d, p)⁴⁴⁻⁴⁷ and MIDI⁴⁸) in order to gain greater insight into the mechanism of the chloroformate/nucleophile-mediated ring cleavage reactions on yohimbine **7** and apovincamine **25**. Our goal was to discern the relationship between this reaction pathway and diastereomeric ratios observed in our experiments using computational tools. As shown in Fig. 5, the tertiary amine of **7** and **25** first reacts with the chloroformate to afford acyl ammonium intermediates, which are primed for the indole-promoted ring cleavage step to afford indole-stabilized carbocation intermediates. We were curious to explore the geometry of possible carbocation intermediates to see if this could potentially dictate the facial selectivity of the subsequent nucleophilic attack from alcohols or thiols, providing the basis for the observed diastereomeric ratios of products.

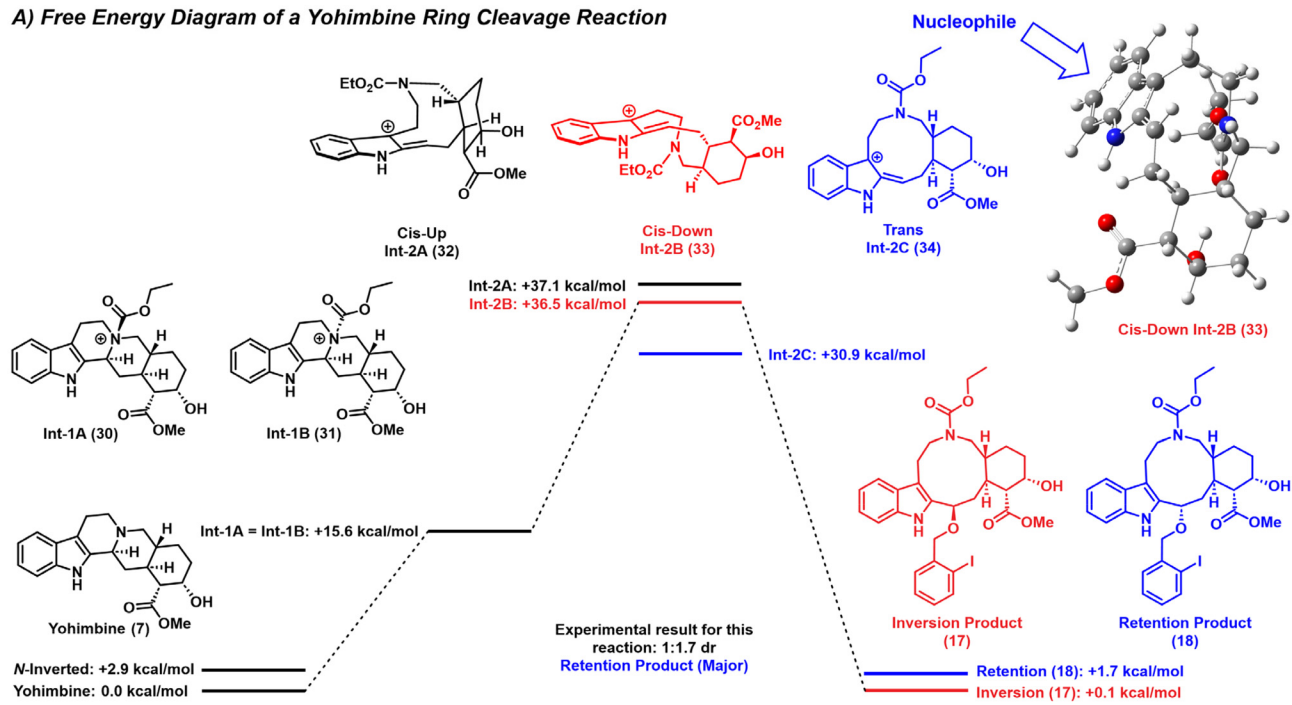
The results for DFT calculations on yohimbine **7** are shown in Fig. 5A and ESI Fig. 8.† Due to the large, complex nature of these compounds, the focus of these calculations was on intermediates rather than assessing potential transition states. Initial data suggested that many local minima and maxima exist, providing a rugged potential energy landscape over the course of this reaction. The intermediates (local minima) shown, however, provide good insight into the reaction pathway. As anticipated, the energetically preferred conformation of yohimbine contains the tertiary amine lone pair of electrons in an axial position, rather than equatorial. The axially-oriented lone pair on the amine of yohimbine (**7**) reacts with ethyl chloroformate to form **Int-1A** (intermediate **30**) preferentially. From there, ring-cleaved carbocations were pro-

posed with either *cis* (structures **32** and **33**) or *trans* (structure **34**) resonance-stabilized geometry. *Trans* carbocation **Int-2C** (structure **34**) was found to have the lowest energy compared to the *cis* intermediates ($\Delta G = +30.9$ kcal mol⁻¹); however, upon C–N bond cleavage, *cis* olefin **33** would initially form. Given that benzylic carbocations have a very high energy barrier to rotation ($\Delta G = 44.9$ kcal mol⁻¹),⁴⁹ it is unlikely that conversion between *cis* **33** and *trans* **34** carbocations occurs after the initial C–N bond cleavage event in this reaction.

Upon closer examination of **Int-1A** (structure **30**), the dihedral angle between the indole NH and the C3 proton is 104.1°, and orbital overlap of the indole pi electrons with the resultant carbocation would favor the formation of a *cis* indole-stabilized carbocation (resonance structures **Int-2A** and **Int-2B**) over a *trans* carbocation. Indeed, upon conducting a relaxed potential energy surface scan wherein the C–N bond of **Int-1A** was incrementally increased in length, it was shown that this proton orients to form a *cis* indole-stabilized carbocation as the bond lengthens before cleavage. Comparing two *cis* carbocation minima in which the carbamate potentially shielded, or blocked, either the top or the bottom face of the reactive center indicated that the latter of the orientations was energetically preferred (**Int-2B** $\Delta G = +36.5$ kcal mol⁻¹ compared to **Int-2A** $\Delta G = +37.1$ kcal mol⁻¹), and this preference was reflected regardless of the solvent model used within the calculation (ESI Fig. 7 and 8†). The combination of the *cis* orientation of the indole-stabilized carbocation and the obstruction of the bottom face from attack due to the position of the carbamate therefore favors the formation of the retention product over the inversion product, indicating kinetic control of product formation over thermodynamic control. This provides a rationale as to why larger nucleophiles, such as 2-iodobenzyl alcohol, preferentially form the retention product, while smaller nucleophiles (e.g., methanol), which are less affected by sterics, form the product diastereomers in roughly a 1:1 ratio from yohimbine. This also provides a rationale as to why ring-cleaved carbamates with larger groups (e.g., phenyl) tend to experience a slightly increased preference for retention products compared to ring-cleaved carbamates with smaller groups (e.g., ethyl). It should be noted, though, that it is possible that there is interconversion between **Int-2B** and **Int-2A** during the course of the reaction as well.

DFT calculations were also conducted for ring cleavage reactions involving apovincamine **25** (Fig. 5B, ESI Fig. 9†). Apovincamine's pentacyclic structure with two chiral centers lends itself to a cup-shaped architecture wherein the tertiary amine's lone pair sits on the convex face of the structure. As a result, it has a strong energetic preference to form the corresponding acyl ammonium intermediate **V-Int-1B** (**36**, $\Delta G = +16.3$ kcal mol⁻¹ compared to **V-Int-1A** **35**, $\Delta G = +24.5$ kcal mol⁻¹) following reaction with phenyl chloroformate. Upon indole-promoted ring cleavage, the newly formed carbamate in **V-Int-2A** (e.g., structure **37**) clearly shields one face of the indole-stabilized carbocation from nucleophilic attack, guiding the formation of the single diastereomer observed (e.g., inversion product **38**). Experimentally, the chloroform-

A) Free Energy Diagram of a Yohimbine Ring Cleavage Reaction



B) Free Energy Diagram of an Apovincamine Ring Cleavage Reaction

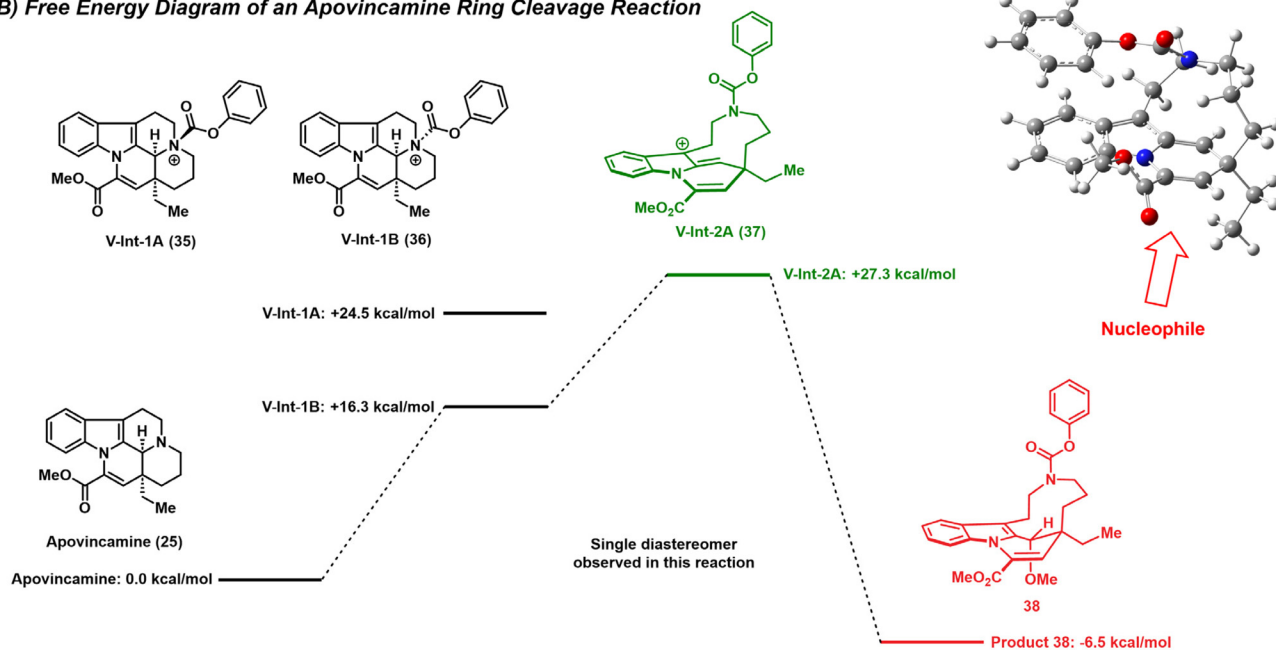


Fig. 5 Free energy diagrams for the chloroformate-mediated ring cleavage reactions of yohimbine 7 and apovincamine 25. (A) Free energy diagram for the ring cleavage pathway of yohimbine reacting with ethyl chloroformate and 2-iodobenzyl alcohol. Optimized structure of Int-2B (33) is shown in the top right of the diagram. (B) Free energy diagram for the ring cleavage pathway of apovincamine reacting with phenyl chloroformate and methanol. Optimized structure of V-Int-2A (37) is shown in the top right of the diagram. Note: The (A) blue and (B) red arrows are pointing to the most accessible face of the (planar) electrophilic center for nucleophilic approach, rationalizing the stereochemical outcome for each reaction.

mate-mediated ring cleavage reaction with apovincamine 25 is low-yielding and significant starting material was observed, which can be rationalized as constrained intermediate V-Int-2A (37) reverting back to starting apovincamine 25 following nitrogen-mediated ring closure to V-Int-1B (36) before final

acyl transfer back to 25 (Fig. 5B). Although the desired product is more energetically favored, the intramolecular cyclization of key intermediate V-Int-2A (37) to apovincamine 25 is likely kinetically favored in this dynamic reactive pathway.

Ring cleavage of reserpine and discovery of re-engineered antiplasmodial agents

Reserpine was subjected to the indole-promoted ring cleavage reaction in the presence of phenyl chloroformate and 2-iodobenzyl alcohol at room temperature for two hours to afford desired diastereomers **40** (5% yield) and **41** (49% yield; Fig. 6A). Despite fewer attempts to develop the chloroformate ring cleavage reaction on reserpine, we observed this indole alkaloid to be highly sensitive to temperature under the reaction conditions utilized for yohimbine. Such chloroformate-based reactions involving reserpine at 60 °C led to decomposition or significant product impurities, likely a result of the electron-rich methoxy group on this indole alkaloid further enhancing reactivity towards the indole-promoted ring cleavage pathway (reactions below room temperature were not explored).

Similar to the C3 position of yohimbine ring-cleaved products, stereochemical validation of the C1 position of these reserpine derivatives was not trivial. While acceptable ¹H and ¹³C NMR spectra could be obtained for diastereomeric products **40** and **41** at room temperature, through-space correlations to this position were more challenging to acquire. The low yields of **40** were exacerbated by the near-coelution of product diastereomers (**40** & **41**); therefore, chromatographic purification was an obstacle. Similar reports by Hoyer⁵⁰ and Seo⁵¹ have documented indole-promoted ring-cleavage reactions of reserpine using alternative reagents. Hoyer and Ross reacted reserpine with a benzyne intermediate to initiate an analogous indole-promoted ring cleavage reaction; however, separation was achieved for only one of the diastereomeric pairs and the stereochemistry at C1 was not determined.⁵⁰ Seo and co-workers reported highly diastereoselective (>20 : 1; 56% yield of the analogous “inversion product” in their study)⁵¹ ring cleavage of reserpine using difluorocarbene transfer chemistry which required 1-D selective NOESY to assign stereochemistry and proved to be critical for our studies with this complex indole alkaloid.

To determine the absolute stereochemistry for **40** and **41**, we performed one-dimensional and two-dimensional NOESY and rotating frame Overhauser effect spectroscopy (ROESY) experiments for each diastereomer. For diastereomer **41** (major product), the stereochemistry at C1 was defined by a key NOE observed between the methyl ester and the C1 proton (Fig. 6A; see ESI† for more details). Through this key NOE, the stereochemistry at C1 of diastereomer **41** was definitively assigned, indicating the “inversion product” is the major product of the reaction, similar to the reaction profile for reserpine observed by Seo and co-workers, who report an analogous NOE to assign the stereochemistry of their major diastereomer formed in their studies.⁵¹

Following the chloroformate-based ring cleavage synthesis efforts, our team screened all compounds for antiplasmodial activity against chloroquine-resistant Dd2 *Plasmodium falciparum* parasites in an unbiased SYBR Green I assay system.^{52–54} While none of the yohimbine- or vincamine-

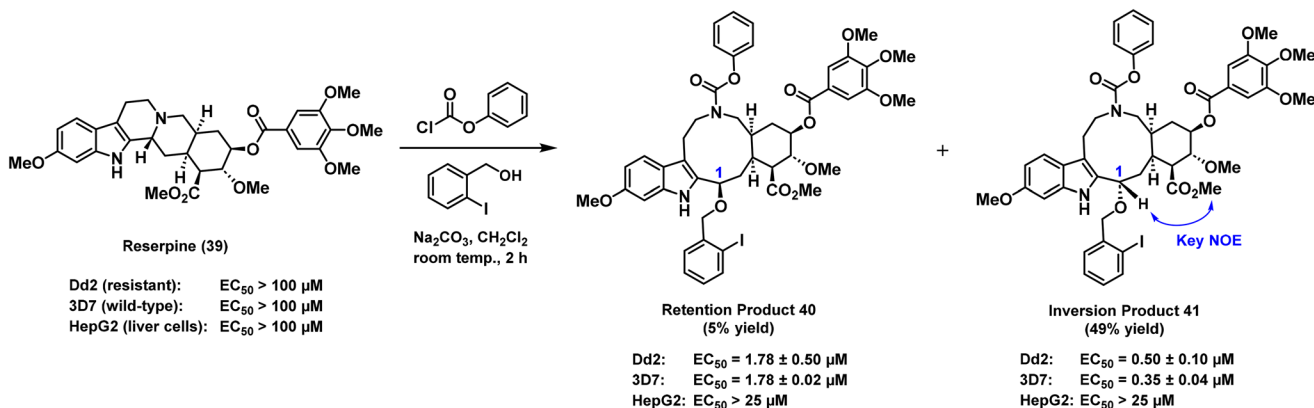
derived compounds exhibited activity in this phenotypic screen against Dd2 parasites, the reserpine-derived compound **41** was found to inhibit 93% of the parasite growth at 1 μM (screening concentration in this study). We then evaluated both reserpine ring-cleavage diastereomers **40** and **41** in dose-response experiments against Dd2 (resistant) and 3D7 (wild-type) parasites for validation of our initial findings and to gain some initial structure-activity relationship (SAR) insights regarding reserpine ring-cleaved diastereomers. From dose-response experiments, we found compound **41** to demonstrate good antiplasmodial activities against Dd2 (EC₅₀ = 0.50 ± 0.10 μM) and 3D7 (EC₅₀ = 0.35 ± 0.04 μM) parasites (Fig. 6A). Interestingly, diastereomer **40** showed a 3- to 5-fold reduction in activity against Dd2 and 3D7 parasites in dose-response experiments (EC₅₀ = 1.78 μM against both strains) compared to **41**.

Importantly, reserpine displayed no inhibitory activities against Dd2 or 3D7 parasites (EC₅₀ > 100 μM) when tested alongside **40** and **41**, demonstrating these ring cleavage efforts to be indeed fruitful as we have re-engineered the biological activity of reserpine. In addition, **40** and **41** were tested for cytotoxicity in HepG2 (hepatocellular carcinoma) cells and found to be inactive (EC₅₀ > 25 μM), demonstrating excellent selectivity indices of >14 and >50 for *P. falciparum* parasites, respectively (selectivity indices were determined by comparing the EC₅₀ value against HepG2 to the EC₅₀ value against Dd2 parasites; [EC₅₀ vs. HepG2]/[EC₅₀ vs. Dd2]). From these initial results against *P. falciparum* parasites and HepG2 cells, compound **41** demonstrates good antiplasmodial activities, and the stereochemistry at C1 is important for activity as can be seen from the loss in activity of analogue **40**.

Following the initial discovery that reserpine-derived compounds **40** and **41** demonstrate re-engineered antiplasmodial activities, we wanted to gain further insights using kill kinetic and stage specific activity assays. Kinetic kill experiments with Dd2 parasites were performed to determine if compounds **40** and **41** were operating through a parasitocidal or parasitostatic mechanism. Asynchronous Dd2 cultures were treated with 10 × EC₅₀ concentration of compounds **40** and **41** for predetermined periods of time (12, 24, and 48 h). Following each time point, compounds **40** and **41** were washed out and parasite growth was evaluated for 96 h. Based on kill kinetic experiments, compounds **40** and **41** required 48 h treatment in Dd2 cultures to demonstrate the most significant reduction in parasitemia. This slow-killing phenotype is indicative of a parasitostatic mode of action, similar to slow-killing antimalarial agent atovaquone (Dihydroartemisinin, or DHA, was used as a rapid-killing agent in kill kinetic experiments; see Fig. 6B). It should be noted that slow-acting antiplasmodial compounds have utility as partner drugs in artemisinin combination therapies.⁵⁵

Finally, we evaluated the developmental stage specific action of compounds **40** and **41** by microscopy and flow cytometry to further explore their activities (Fig. 7). The precise delineation regarding the timing of action for a small molecule can provide valuable insights into the developmental growth and clinical clearance of *P. falciparum*. For these experiments,

A) Indole-Promoted Ring Cleavage of Reserpine Leads to Re-engineered Antiparasmodial Agents



B) Kill Kinetics against *P. falciparum* Dd2 Parasites

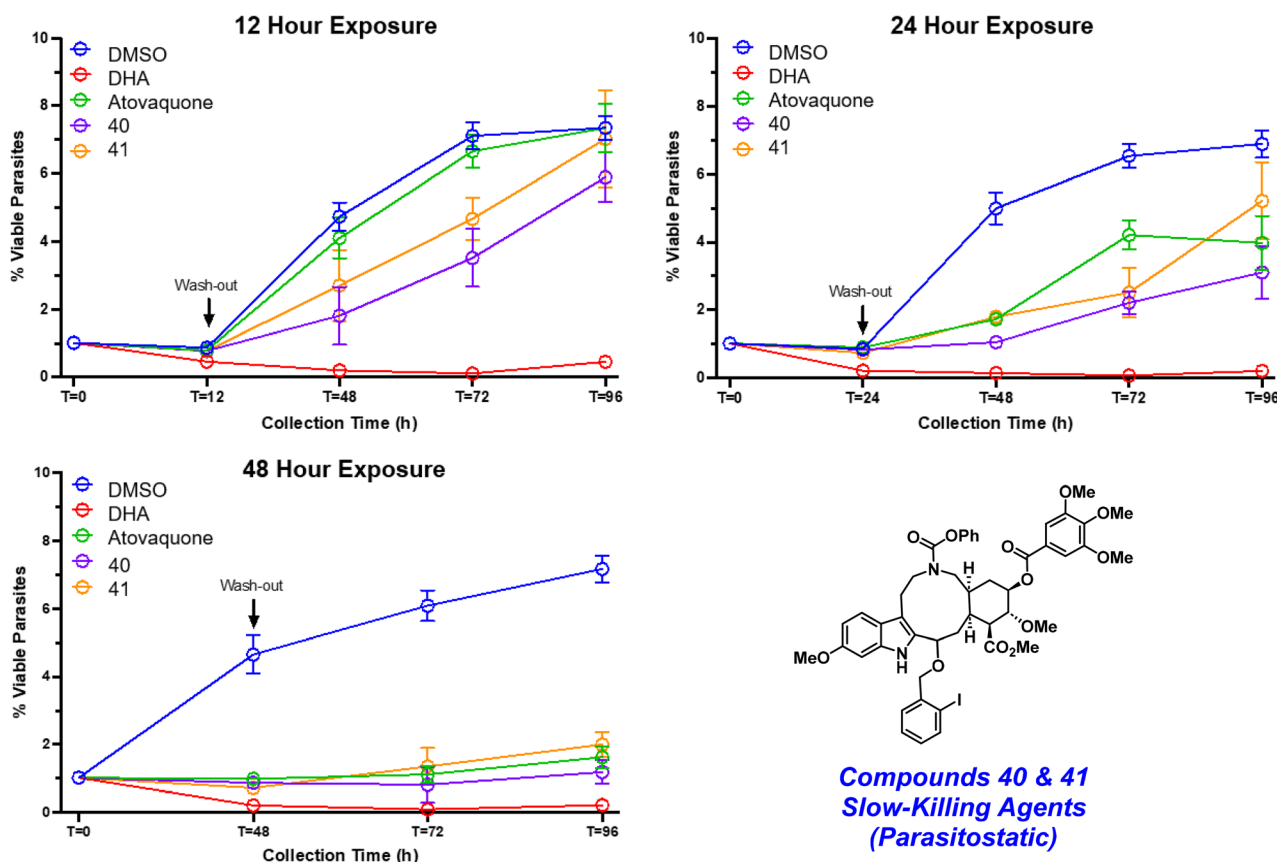


Fig. 6 (A) Indole-promoted ring cleavage of reserpine delivers new antiplasmodial agents. Key NOE correlations for stereochemical assignment of **41** are included. (B) Kinetic kill experiments of *P. falciparum* Dd2 cultures demonstrate **40** and **41** to be parasitostatic agents. Compounds were added at $10 \times EC_{50}$ concentrations to synchronous Dd2 culture at 1% parasitemia and 4% hematocrit starting at 6 hours post invasion (HPI). Dd2 culture was synchronized by using 5% sorbitol. Cultures were exposed to the compound of interest during 12, 24, and 48 h, followed by washing steps and continuous monitoring of parasite regrowth over the course of four days. PBS and 0.5% BSA were used for washing and blocking steps. Samples were collected every 24 h until the 96 h time point. A combination of Mitotracker Deep red (MTDR) and SYBR Green I dyes were used to stain mitochondrial content in live parasites and parasitemia, respectively. Uninfected red blood cells and no mitotracker controls were used to assist with flow-cytometry analysis. Dimethyl sulfoxide (DMSO) was used as a negative control. Dihydroartemisinin (DHA) was used as a positive control for rapid parasite killing (parasitocidal action), and atovaquone was also used as a positive control for slow parasite killing (parasitostatic action). GraphPad Prism was used to analyze the flow cytometry data. Results are expressed as the means of triplicate biological experiments and parasite viability.

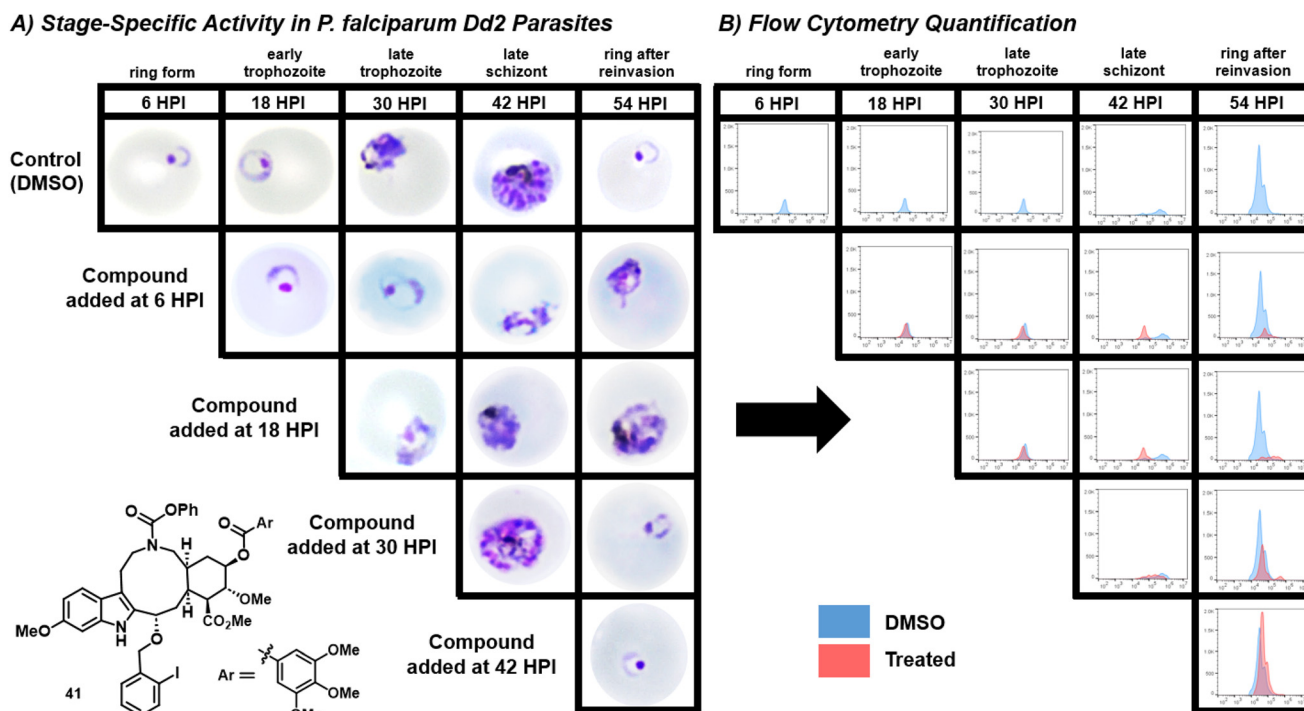


Fig. 7 Stage-specific activity of **41** in *P. falciparum* Dd2 parasites. Dd2 culture was synchronized by using 5% sorbitol. The culture was then diluted to 1% parasitemia and 2% hematocrit. Compounds of interest were added at $5 \times EC_{50}$ concentrations at 6, 18, 30 and 42 HPI. DMSO and DHA were used as a negative and positive controls, respectively. Samples were collected every 12 h at every stage until reinvasion at 54 HPI. Giemsa smearing was used to observe the parasite morphology, and flow cytometry was used to observe parasite DNA content. Samples were fixed in 4% paraformaldehyde, and PBS was used for washing steps. Samples were permeabilized in 0.25% Triton X-100 and stained using DNA dye YOYO-1. FlowJo (v 10.8) was used to analyze the flow cytometry data. Results are representative of triplicate biological experiments.

tightly synchronized Dd2 cultures were treated at 6 hours post-invasion of merozoites with $5 \times EC_{50}$ concentration of compounds **40** and **41**. Following this, microscopic evaluation of Giemsa-stained-thin smears and flow cytometric assessments were performed at 12 h intervals. Negative controls represented infected red blood cells that were exposed to vehicle (0.1% DMSO) only. When compared to untreated Dd2 cultures, compounds **40** and **41** inhibited parasites later in the life cycle between the trophozoite and schizogony stages (compound **41** shown in Fig. 7; analogous stage specific action experiments are reported for compound **40** in the ESI†). Compound **41** prevented reinvasion (Fig. 7A) and increases in parasitemia (Fig. 7B) when added to Dd2 cultures 18 h post-invasion (HPI). In addition, we note that **41** caused vacuolization in the schizont stage parasites, which do not overlap with heme, distinguishing these newly formed vacuoles from the digestive vacuole in *P. falciparum*. When **40** and **41** were added to Dd2 cultures 30 HPI, both reinvasion and increases in parasite mass were not altered as these compounds do not operate this late in the parasite's life cycle.

Conclusions

During these studies, we demonstrated multiple indole alkaloids to be viable substrates for a chloroformate-mediated ring

cleavage reaction in combination with alcohol/thiol nucleophiles. This robust reaction was most explored with yohimbine **7**, which formed two diastereomeric products under moderate reaction conditions; however, extensive NMR studies in combination with five X-rays were required to define the absolute stereochemistry for the corresponding ring-cleaved products. Apovincamine **25** and vinburnine **28** were also utilized as substrates; however, these molecules were less ideal starting materials as they afforded significantly lower yields of the desired product (formed as a single diastereomer). Free energy calculations were utilized to define the energetics of this indole-promoted reaction pathway to better understand our experimental findings with yohimbine **7** and apovincamine **25**. In addition, we explored this chloroformate-based reaction with reserpine **39**, which was sensitive to elevated temperatures, but proceeded well at room temperature to produce two diastereomeric products (requiring NOE to determine the stereochemistry of **41**). This focused collection of ring-cleaved indole alkaloid derived compounds was screened for activity against Dd2 *P. falciparum* parasites, and we identified compounds **40** and **41** (from reserpine) to demonstrate re-engineered antiplasmodial activities. With our initial findings reported herein, tool compounds **40** and **41** have already demonstrated new insights and encourage further explorations (*i.e.*, target identification) to better understand *P. falciparum* biology. Overall, these studies demonstrate the Complexity-to-

Diversity approach using indole alkaloids as starting points can lead to interesting and diverse compound collections with re-engineered biological activities in significant disease areas related to human health.

Data availability

Synthesis procedures, ^1H and ^{13}C NMR data, X-ray data, computational analysis methods and data, antiplasmodial procedures and results, and NMR spectra including select 2-D (e.g., COSY, HSQC) NMR spectra are available in the ESI.†

Author contributions

R. W. H. directed this study and coordinated collaborative efforts with D. C. (antimalarial studies) and C. L. (computational studies). D. C. S. performed calculations studies, carried out extensive NMR data analysis of the synthesized compounds, and wrote the manuscript draft. A. C. R. carried out nearly all reported yohimbine ring cleavage reactions, obtained X-rays for **18**, **20**, **22**, **24**, and initially worked on the reserpine ring cleavage reaction. M. G. G. carried out all reported apovincamine ring cleavage reactions, obtained X-rays for **14** and **27**, and assisted with characterizing new compounds (NMR analysis). B. R. B. optimized the ring cleavage reaction on reserpine (and purification of **40** and **41**), defined the stereochemistry of **41** using extensive NMR experiments, and assisted in drafting the manuscript. R. A. P. and N. M. S. performed the biological studies that led to the discovery of antiplasmodial agents **40** and **41**. S. T. synthesized a few yohimbine derivatives and carried out the ring cleavage reaction on vinburnine. K. A. A. generated X-ray data during these studies. J. R. R. was critical to guiding and optimizing the extensive NMR studies reported herein. G. S. provided critical guidance with Gaussian and HiPerGator (computational work). C. L. directed the computational studies to better understand the stereochemical outcomes of the ring cleavage reactions. D. C. directed the antiplasmodial studies of **40** and **41**. R. W. H. guided the chemical synthesis efforts, performed the final NMR data review, and finalized manuscript writing with several co-authors, primarily D. C. and D. C. S. All authors have reviewed and agree with the scientific findings reported in this manuscript.

Conflicts of interest

The authors declare no conflicts of interest.

Acknowledgements

We acknowledge the University of Florida, the National Institute of General Medical Sciences for providing generous support for this work (R35GM128621 to R. W. H.), and the

National Cancer Institute (R01CA212403 to C. L.). D. C. S. was partially supported by a Graduate Student Fellowship from the University of Florida. A. C. R. was partially supported by a postdoctoral fellowship from CONACYT (CVU No: 346860). M. G. G. was supported by the NIH/NIGMS T32GM136583 “Chemistry-Biology Interface Training Program” at the University of Florida. B. B. was supported by the NIH-NIDCR training grant T90 DE021990 “Comprehensive Training Program in Oral Biology” at the University of Florida. We would like to thank Dr Ion Ghiviriga and Robert Harker (UF Chemistry) for assistance with NMR experiments. A portion of this work was performed in the McKnight Brain Institute at the National High Magnetic Field Laboratory’s Advanced Magnetic Resonance Imaging and Spectroscopy (AMRIS) Facility, which is supported by National Science Foundation Cooperative Agreement DMR-1644779 and the State of Florida. We thank the NSF for funding of the X-ray diffractometer at the Center for X-ray Crystallography at the University of Florida through grant CHE-1828064. High resolution mass spectra were obtained for novel synthesized compounds from the University of Florida’s Mass Spectrometry Research and Education Center (supported by NIH S10 OD021758-01A1). Gaussian calculations were performed using HiPerGator 2.0 and 3.0, and we acknowledge University of Florida Research Computing for providing computational resources and support that have contributed to the results reported herein.

References

- 1 R. W. Huigens III, K. C. Morrison, R. W. Hicklin, T. A. Flood Jr, M. F. Richter and P. J. A. Hergenrother, Ring-Distortion Strategy to Construct Stereochemically Complex and Structurally Diverse Compounds from Natural Products, *Nat. Chem.*, 2013, **5**, 195–202.
- 2 R. W. Hicklin, T. L. López Silva and P. J. Hergenrother, Synthesis of Bridged Oxafenestranes from Pleuromutilin, *Angew. Chem., Int. Ed.*, 2014, **53**, 9880–9883.
- 3 N. G. Paciaroni, D. L. Perry, V. M. Norwood, C. Murillo-Solano, J. Collins, S. Tenneti, D. Chakrabarti and R. W. Huigens III, Re-Engineering, of Yohimbine’s Biological Activity through Ring Distortion: Identification and Structure–Activity Relationships of a New Class of Antiplasmodial Agents, *ACS Infect. Dis.*, 2020, **6**, 159–167.
- 4 V. M. Norwood, C. Murillo-Solano, M. G. Goertzen, B. R. Brummel, D. L. Perry, J. R. Rocca, D. Chakrabarti and R. W. Huigens III, Ring Distortion of Vincamine Leads to the Identification of Re-Engineered Antiplasmodial Agents, *ACS Omega*, 2021, **6**, 20455–20470.
- 5 V. Srinivasulu, G. Srikanth, M. A. Khanfar, I. A. Abu-Yousef, A. F. Majdalawieh, R. Mazitschek, S. C. Setty, A. Sebastian and T. H. Al-Tel, Stereodivergent Complexity-to-Diversity Strategy En Route to the Synthesis of Nature-Inspired Skeleta, *J. Org. Chem.*, 2022, **87**, 1377–1397.
- 6 N. G. Paciaroni, V. M. Norwood, R. Ratnayake, H. Luesch and R. W. Huigens III, Yohimbine as a Starting Point to

- Access Diverse Natural Product-Like Agents with Re-Programmed Activities against Cancer-Relevant GPCR Targets, *Bioorg. Med. Chem.*, 2020, **28**, 115546.
- 7 R. W. Huigens III, N. G. Paciaroni and H. Luesch, Analogs of Yohimbine and Uses Thereof, US2019256490A1, 2019.
- 8 R. W. Huigens III, V. M. Norwood and H. Luesch, Analogs of Vincamine and Uses Thereof, US2019359622A1, 2019.
- 9 R. J. Rafferty, R. W. Hicklin, K. A. Maloof and P. J. Hergenrother, Synthesis of Complex and Diverse Compounds through Ring Distortion of Abietic Acid, *Angew. Chem., Int. Ed.*, 2014, **53**, 220–224.
- 10 A. Garcia, B. S. Drown and P. J. Hergenrother, Access to a Structurally Complex Compound Collection via Ring Distortion of the Alkaloid Sinomenine, *Org. Lett.*, 2016, **18**, 4852–4855.
- 11 N. G. Paciaroni, R. Ratnayake, J. H. Matthews, V. M. Norwood, A. C. Arnold, L. H. Dang, H. Luesch and R. W. Huigens III, Tryptoline Ring-Distortion Strategy Leads to Complex and Diverse Biologically Active Molecules from the Indole Alkaloid Yohimbine, *Chem. – Eur. J.*, 2017, **23**, 4327–4335.
- 12 S. Z. Tasker, A. E. Cowfer and P. J. Hergenrother, Preparation of Structurally Diverse Compounds from the Natural Product Lycorine, *Org. Lett.*, 2018, **20**, 5894–5898.
- 13 M. Charaschanya and J. Aubé, Reagent-Controlled Regiodivergent Ring Expansions of Steroids, *Nat. Commun.*, 2018, **9**, 934.
- 14 C. Zhao, Z. Ye, Z. Ma, S. A. Wildman, S. A. Blaszczyk, L. Hu, I. A. Guizei and W. Tang, A General Strategy for Diversifying Complex Natural Products to Polycyclic Scaffolds with Medium-Sized Rings, *Nat. Commun.*, 2019, **10**, 4015.
- 15 E. Llabani, R. W. Hicklin, H. Y. Lee, S. E. Motika, L. A. Crawford, E. Weerapana and P. J. Hergenrother, Diverse Compounds from Pleuromutilin Lead to a Thioredoxin Inhibitor and Inducer of Ferroptosis, *Nat. Chem.*, 2019, **11**, 521–532.
- 16 V. M. Norwood, A. C. Brice-Tutt, S. O. Eans, H. M. Stacy, G. Shi, R. Ratnayake, J. R. Rocca, K. A. Abboud, C. Li, H. Luesch, J. P. McLaughlin and R. W. Huigens III, Preventing Morphine-Seeking Behavior through the Re-Engineering of Vincamine's Biological Activity, *J. Med. Chem.*, 2020, **63**, 5119–5138.
- 17 S. Shang and D. S. Tan, Advancing Chemistry and Biology through Diversity-Oriented Synthesis of Natural Product-like Libraries, *Curr. Opin. Chem. Biol.*, 2005, **9**, 248–258.
- 18 S. L. Schreiber, Molecular Diversity by Design, *Nature*, 2009, **457**, 153–154.
- 19 W. R. J. D. Galloway, A. Isidro-Llobet and D. R. Spring, Diversity-Oriented Synthesis as a Tool for the Discovery of Novel Biologically Active Small Molecules, *Nat. Commun.*, 2010, **1**, 80.
- 20 C. J. Gerry and S. L. Schreiber, Chemical Probes and Drug Leads from Advances in Synthetic Planning and Methodology, *Nat. Rev. Drug Discovery*, 2018, **17**, 333–352.
- 21 S. L. Schreiber, Target-Oriented and Diversity-Oriented Organic Synthesis in Drug Discovery, *Science*, 2000, **287**, 1964–1969.
- 22 M. D. Burke and S. L. Schreiber, A Planning Strategy for Diversity-Oriented Synthesis, *Angew. Chem., Int. Ed.*, 2004, **43**, 46–58.
- 23 C. J. Gerry and S. L. Schreiber, Recent Achievements and Current Trajectories of Diversity-Oriented Synthesis, *Curr. Opin. Chem. Biol.*, 2020, **56**, 1–9.
- 24 R. J. Spandl, M. Díaz-Gavilán, K. M. G. O'Connell, G. L. Thomas and D. R. Spring, Diversity-oriented Synthesis, *Chem. Rec.*, 2008, **8**, 129–142.
- 25 H. van Hattum and H. Waldmann, Biology-Oriented Synthesis: Harnessing the Power of Evolution, *J. Am. Chem. Soc.*, 2014, **136**, 11853–11859.
- 26 S. Wetzel, R. S. Bon, K. Kumar and H. Waldmann, Biology-Oriented Synthesis, *Angew. Chem., Int. Ed.*, 2011, **50**, 10800–10826.
- 27 J. Švenda, M. Sheremet, L. Kremer, L. Maier, J. O. Bauer, C. Strohmam, S. Ziegler, K. Kumar and H. Waldmann, Biology-Oriented Synthesis of a Withanolide-Inspired Compound Collection Reveals Novel Modulators of Hedgehog Signaling, *Angew. Chem., Int. Ed.*, 2015, **54**, 5596–5602.
- 28 M. Sheremet, S. Kapoor, P. Schröder, K. Kumar, S. Ziegler and H. Waldmann, Small Molecules Inspired by the Natural Product Withanolides as Potent Inhibitors of Wnt Signaling, *ChemBioChem*, 2017, **18**, 1797–1806.
- 29 G. Karageorgis and H. Waldmann, Guided by Evolution: Biology-Oriented Synthesis of Bioactive Compound Classes, *Synthesis*, 2019, **51**, 55–66.
- 30 T. Schneidewind, S. Kapoor, G. Garivet, G. Karageorgis, R. Narayan, G. Vendrell-Navarro, A. P. Antonchick, S. Ziegler and H. Waldmann, The Pseudo Natural Product Myokinasib Is a Myosin Light Chain Kinase 1 Inhibitor with Unprecedented Chemotype, *Cell Chem. Biol.*, 2019, **26**, 512–523.
- 31 G. S. Cremosnik, J. Liu and H. Waldmann, Guided by Evolution: From Biology Oriented Synthesis to Pseudo Natural Products, *Nat. Prod. Rep.*, 2020, **37**, 1497–1510.
- 32 W. Wilk, T. J. Zimmermann, M. Kaiser and H. Waldmann, Principles, Implementation, and Application of Biology-Oriented Synthesis (BIOS), *Biol. Chem.*, 2010, **391**, 491–497.
- 33 S.-I. Sakai, A. Kubo, K. Katano, N. Shinma and K. Sasago, Transformation of Indole Alkaloids. II. On the C/D Ring Opening and Closing Reactions of Indole Alkaloids and the Syntheses of Vobasine Type Alkaloids, *Yakugaku Zasshi*, 1973, **93**, 1165–1182.
- 34 S. Mahboobi, W. Wagner, T. Burgemeister and W. Wiegrebe, Non-Identity of Nazlinin and 6- Azacyclodeca [5,4-b]Indol-1-Amine, *Arch. Pharm.*, 1994, **327**, 463–465.
- 35 C. T. Liu, S. C. Sun and Q. S. Yu, Synthesis and Photooxidation of the Condensation Products of Tryptamine and Catechol Derivatives. An Approach to the Synthesis of a Probable Precursor of Koumine, *J. Org. Chem.*, 1983, **48**, 44–47.
- 36 D. A. Leas, D. C. Schultz and R. W. Huigens III, Chemical Reactions of Indole Alkaloids That Enable Rapid Access to New Scaffolds for Discovery, *SynOpen*, 2023, **7**, 165–185.
- 37 P. Magnus, M. Giles, R. Bonnert, G. Johnson, L. McQuire, M. Deluca, A. Merritt, C. S. Kim and N. Vicker, Synthesis of

- Strychnine and the Wieland-Gumlich Aldehyde, *J. Am. Chem. Soc.*, 1993, **115**, 8116–8129.
- 38 A. Guerriero, M. D'Ambrosio and F. Pietra, Slowly Interconverting Conformers of The Briarane Diterpenoids Verecynarmin B, C, and D, Isolated from the Nudibranch Mollusc *Armina Maculata* and the Pennatulacean Octocoral *Veretillum Cynomorium* of East Pyrenean Waters, *Helv. Chim. Acta*, 1988, **71**, 472–485.
- 39 A. D. Bain, R. A. Bell, D. A. Fletcher, P. Hazendonk, R. A. Maharajh, S. Rigby and J. F. Valliant, NMR Studies of Chemical Exchange amongst Five Conformers of a Ten-Membered Ring Compound Containing Two Amide Bonds and a Disulfide, *J. Chem. Soc., Perkin Trans. 2*, 1999, 1447–1454.
- 40 T. Lebl, M. M. Lorion, A. M. Jones, D. Philp and N. J. Westwood, Synthesis and Characterisation of Medium-Sized Ring Systems by Oxidative Cleavage. Part 2: Insights from the Study of Ring Expanded Analogues, *Tetrahedron*, 2010, **66**, 9694–9702.
- 41 M. J. Frisch, G. W. Trucks, H. B. Schlegel, G. E. Scuseria, M. A. Robb, J. R. Cheeseman, G. Scalmani, V. Barone, B. Mennucci, G. A. Petersson, H. Nakatsuji, M. Caricato, X. Li, H. P. Hratchian, A. F. Izmaylov, J. Bloino, G. Zheng, J. L. Sonnenberg, M. Hada, M. Ehara, K. Toyota, R. Fukuda, J. Hasegawa, M. Ishida, T. Nakajima, Y. Honda, O. Kitao, H. Nakai, T. Vreven, J. A. Montgomery Jr., J. E. Peralta, F. Ogliaro, M. Bearpark, J. J. Heyd, E. Brothers, K. N. Kudin, V. N. Staroverov, R. Kobayashi, J. Normand, K. Raghavachari, A. Rendell, J. C. Burant, S. S. Iyengar, J. Tomasi, M. Cossi, N. Rega, J. M. Millam, M. Klene, J. E. Knox, J. B. Cross, V. Bakken, C. Adamo, J. Jaramillo, R. Gomperts, R. E. Stratmann, O. Yazyev, A. J. Austin, R. Cammi, C. Pomelli, J. W. Ochterski, R. L. Martin, K. Morokuma, V. G. Zakrzewski, G. A. Voth, P. Salvador, J. J. Dannenberg, S. Dapprich, A. D. Daniels, Ö. Farkas, J. B. Foresman, J. V. Ortiz, J. Cioslowski and D. J. Fox, *Gaussian 09, Revision D.01*, Gaussian, Inc., Wallingford CT, 2013.
- 42 M. J. Frisch, G. W. Trucks, H. B. Schlegel, G. E. Scuseria, M. A. Robb, J. R. Cheeseman, G. Scalmani, V. Barone, G. A. Petersson, H. Nakatsuji, X. Li, M. Caricato, A. V. Marenich, J. Bloino, B. G. Janesko, R. Gomperts, B. Mennucci, H. P. Hratchian, J. V. Ortiz, A. F. Izmaylov, J. L. Sonnenberg, D. Williams-Young, F. Ding, F. Lipparini, F. Egidi, J. Goings, B. Peng, A. Petrone, T. Henderson, D. Ranasinghe, V. G. Zakrzewski, J. Gao, N. Rega, G. Zheng, W. Liang, M. Hada, M. Ehara, K. Toyota, R. Fukuda, J. Hasegawa, M. Ishida, T. Nakajima, Y. Honda, O. Kitao, H. Nakai, T. Vreven, K. Throssell, J. A. Montgomery Jr., J. E. Peralta, F. Ogliaro, M. J. Bearpark, J. J. Heyd, E. N. Brothers, K. N. Kudin, V. N. Staroverov, T. A. Keith, R. Kobayashi, J. Normand, K. Raghavachari, A. P. Rendell, J. C. Burant, S. S. Iyengar, J. Tomasi, M. Cossi, J. M. Millam, M. Klene, C. Adamo, R. Cammi, J. W. Ochterski, R. L. Martin, K. Morokuma, O. Farkas, J. B. Foresman and D. J. Fox, *Gaussian 16, Revision C.01*, Gaussian, Inc., Wallingford CT, 2019.
- 43 Y. Zhao and D. G. Truhlar, The M06 Suite of Density Functionals for Main Group Thermochemistry, Thermochemical Kinetics, Noncovalent Interactions, Excited States, and Transition Elements: Two New Functionals and Systematic Testing of Four M06-Class Functionals and 12 Other Function, *Theor. Chem. Acc.*, 2008, **120**, 215–241.
- 44 R. Krishnan, J. S. Binkley, R. Seeger and J. A. Pople, Self-consistent Molecular Orbital Methods. XX. A Basis Set for Correlated Wave Functions, *J. Chem. Phys.*, 1980, **72**, 650–654.
- 45 A. D. McLean and G. S. Chandler, Contracted Gaussian Basis Sets for Molecular Calculations. I. Second Row Atoms, $Z = 11-18$, *J. Chem. Phys.*, 1980, **72**, 5639–5648.
- 46 T. Clark, J. Chandrasekhar, G. W. Spitznagel and P. V. R. Schleyer, Efficient Diffuse Function-Augmented Basis Sets for Anion Calculations. III. The 3–21 + G Basis Set for First-Row Elements, Li–F, *J. Comput. Chem.*, 1983, **4**, 294–301.
- 47 M. J. Frisch, J. A. Pople and J. S. Binkley, Self-consistent Molecular Orbital Methods 25. Supplementary Functions for Gaussian Basis Sets, *J. Chem. Phys.*, 1984, **80**, 3265–3269.
- 48 R. E. Easton, D. J. Giesen, A. Welch, C. J. Cramer and D. G. Truhlar, The MIDI! Basis Set for Quantum Mechanical Calculations of Molecular Geometries and Partial Charges, *Theor. Chim. Acta*, 1996, **93**, 281–301.
- 49 Z. Li, T. Bally, K. N. Houk and W. T. Borden, Variations in Rotational Barriers of Allyl and Benzyl Cations, Anions, and Radicals, *J. Org. Chem.*, 2016, **81**, 9576–9584.
- 50 S. P. Ross and T. R. Hoye, Reactions of Hexadecylo-Diels–Alder Benzynes with Structurally Complex Multifunctional Natural Products, *Nat. Chem.*, 2017, **9**, 523–530.
- 51 Y. Kim, J. Heo, D. Kim, S. Chang and S. Seo, Ring-Opening Functionalizations of Unstrained Cyclic Amines Enabled by Difluorocarbene Transfer, *Nat. Commun.*, 2020, **11**, 4761.
- 52 M. Smilkstein, N. Sriwilajjaroen, J. X. Kelly, P. Wilairat and M. Riscoe, Simple and Inexpensive Fluorescence-Based Technique for High-Throughput Antimalarial Drug Screening, *Antimicrob. Agents Chemother.*, 2004, **48**, 1803–1806.
- 53 T. N. Bennett, M. Paguio, B. Gligorijevic, C. Seudieu, A. D. Kosar, E. Davidson and P. D. Roepe, Novel, Rapid, and Inexpensive Cell-Based Quantification of Antimalarial Drug Efficacy, *Antimicrob. Agents Chemother.*, 2004, **48**, 1807–1810.
- 54 J. D. Johnson, R. A. Denuff, L. Gerena, M. Lopez-Sanchez, N. E. Roncal and N. C. Waters, Assessment and Continued Validation of the Malaria SYBR Green I-Based Fluorescence Assay for use in Malaria Drug Screening, *Antimicrob. Agents Chemother.*, 2007, **51**, 1926–1933.
- 55 N. Erhunse and D. Sahal, Protecting Future Antimalarials from the Trap of Resistance: Lessons from Artemisinin-based Combination Therapy (ACT) Failures, *J. Pharm. Anal.*, 2021, **11**, 541–554.